Journal of GeoEngineering, Vol. 11, No. 1, pp. 1-12, April 2016
http://dx.doi.org/10.6310/jog.2016.11(1).1

2015 TGS Geotechnical Lecture:
FINITE ELEMENT ANALYSIS OF DEEP EXCAVATION PROBLEMS

Chang-Yu Ou [1]

ABSTRACT

The finite element method is a powerful tool for the analysis of deep excavation problems. Since soil is a highly nonlinear, plastic and porewater pressure dependent material, to realistically predict the deformation of soil, rational formulation of constitutive models and flow rules are necessary. This paper presents the commonly used constitutive soil models suitable for the analysis of deep excavation problems where the input parameters can be derived from the basic soil properties in the effective stress drained and undrained analyses. Moreover, the total stress undrained analysis was an alternative for the undrained clay where the stiffness of the undrained clay has to be obtained from empirical formulae. The finite element method can also be used for the analysis of stability problems. With the inclusion of elastic-plastic properties of structure members in the analysis and simulation of center posts in excavations, the finite element analysis can result in good estimate the factor of safety of excavations. Finally the three dimensional finite element analysis of excavations with buttress walls was presented to demonstrate its applicability. It is found that the wall deflection and ground settlement for excavations with buttress walls can be well predicted. The mechanism of buttress walls in reducing the lateral wall deflection can also be understood. Design of buttress walls in excavations would be more reasonable.

Key words: Effective stress undrained analysis, total stress undrained analysis, stress paths, deformation analysis, stability analysis, three dimensional analysis.

1. INTRODUCTION

Design of an excavation necessarily considers its stability and serviceability. The former concerns the safety of the excavation system and the latter aims to avoid the damage of adjacent properties such as buildings and public utilities. In the past several simple formulae for stability analysis (*e.g.*, Terzaghi 1943; Bjerrum and Eide 1956; JSA 1988; Tschebotarioff 1951; Hsieh *et al*. 2008) have been developed based on theory of bearing capacity or limiting equilibrium, with little consideration of the entire structural system. Moreover, many empirical methods (*e.g.*, Bowles 1986; Clough and O'Rourke 1990; Hsieh and Ou 1998; Osman and Bolton 2006; Ou and Hsieh 2011; Hsieh and Ou 2016; Peck 1969) have also been derived to estimate the amount of deflection of retaining walls and ground settlement. Those methods were basically derived from the monitoring results of excavation case histories, representing the effects of every relevant element on deformation. Normally it can lead to effective predictions, without much complexity, for similar excavation projects, in terms of soil conditions, construction methods, and engineering design. Nevertheless, those predictions are only applicable to normal excavations. For some excavations with special designs such as ground improvement, installation of cross walls and buttress walls, or mixed top-down with bottom-up excavations, the prediction from empirical methods may lead to inaccurate results.

The stability and movements of an excavation are engendered by unbalanced forces acting on the wall due to the removal of soils within the excavation zone. The magnitude of unbalanced forces is influenced by many factors: the conditions of soil layers, the level and pressures of groundwater, the excavation depth, the excavation width and so on. The finite element method is capable of simulating these factors and therefore the results derived from the method would be more accurate than those derived from simple stability formulae and empirical methods. Therefore, the finite element method has been applied to the analysis of deep excavation problems quite extensively.

It is generally understood that the accuracy of the finite element method depends on the formulation of constitutive models and selection of soil parameters. Since the stress strain behavior of soil is highly non-linear, anisotropic, porewater pressure dependent, and plastic, the formulation of constitutive models is usually very complicated. Moreover, the selection of soil parameters (*e.g.,* strength and stiffness parameters) is a crucial step in the finite element analysis. A common problem in the analysis of deep excavations is that the soil tests data are often limited or of low-quality due to the difficulty in taking undisturbed in situ samples.

The objective of this paper is to present the commonly used analysis methodology of the finite element method including total stress analysis and effective stress analysis for clay, constitutive model, deformation analysis and stability analysis. Finally, the three dimensional (3D) analysis will be elucidated to address the importance of the 3D behavior of excavations.

2. EFFECTIVE AND TOTAL STRESS ANALYSES

In the geotechnical analysis the geomaterial must be classified as either drained or undrained material. Drained material

Manuscript received March 10, 2016; revised March 14, 2016; accepted March 15, 2016.
[1] Professor (corresponding author), Department of Civil and Construction Engineering, National Taiwan University of Science and Technology, Taipei, Taiwan (e-mail: ou@mail.ntust.edu.tw).

certainly needs to be analyzed with effective stress analysis in which excess porewater pressure is set equal to 0. There are two types of undrained analysis, namely, total stress undrained analysis and effective stress undrained analysis.

In the total stress undrained analysis, the soil and water are treated as a single material and the ground water level is set at the bottom of the finite element mesh to avoid the influence of ground water on the soil and structure in the analysis. All the parameters of soil should be expressed in terms of total stress, for example, strength parameters (c, $\phi = 0$), undrained Young's modulus (E_u) and undrained Poisson's ratio ($\mu = 0.495$). The coefficient of the at-rest earth pressure is equal to 1.0. The parameters of the material used in the analysis are not intrinsic properties because they are affected by the development of excess porewater pressure that does not appear in the analysis. Therefore, the parameters derived or measured from laboratory or field tests should be with the same stress path as those in the field condition to ensure a similar development of excess porewater pressure. Although the strength parameters can be measured from the unconsolidated undrained test or vane shear test, the undrained Young's modulus can only be estimated from empirical formulae.

In the effective stress undrained analysis, soil and water are treated as two phases and the actual location of ground water level should be set. All the parameters of soil are expressed in terms of effective parameters, for example, effective strength parameters (c' and ϕ'), effective Young's modulus (E') and effective Poisson's ratio (μ'), *etc*., The coefficient of the at-rest earth pressure should be conformed with the geostatic condition. Most importantly, the stresses computed from the finite element method are affected by the generation of excess porewater pressure that can be computed from the finite element computation procedure. The procedure for the effective stress undrained analysis can be summarized as

1. Input the effective stress parameters (*e.g.*, c', ϕ', E' and μ'), compute the constitutive stiffness matrix of soil $[D']$
2. Input water stiffness, compute the constitutive stiffness matrix of porewater $[D_f]$
3. Compute $[D] = [D'] + [D_f]$, then form the element stiffness matrix $[K_E]$
4. Assemble the $[K_E]$ into global stiffness matrix $[K_G]$
5. Use the standard finite element procedure $[R] = [K_G][d_n]$ to compute nodal displacements $[d_n]$ where $[R]$ is nodal forces
6. Through $\{\varepsilon\} = [B][d_n]$ to compute strain in an element $\{\varepsilon\}$
7. Through $\{\sigma'\} = [D']\ \{\varepsilon\}$ to obtain the effective stress $\{\sigma'\}$
8. Through $\{\sigma_f\} = [D_f]\ \{\varepsilon\}$ to yield the porewater pressure $\{\sigma_f\}$

3. CONSTITUTIVE SOIL MODEL AND ITS APPLICATION

In an excavation, the stress alteration associated with vertical and horizontal stress relief is very complex. It depends on several factors, such as type of retaining wall, excavation depth, stress history of soil, *etc*. Figure 1 illustrates possible stress paths in an excavation from the result of finite element analysis (Ng 1999). As we understand, the stress strain response of soil is stress path dependent and to realistically simulate the deformation behavior of soil, good constitutive models are certainly required. As mentioned in the proceeding section, the behavior of

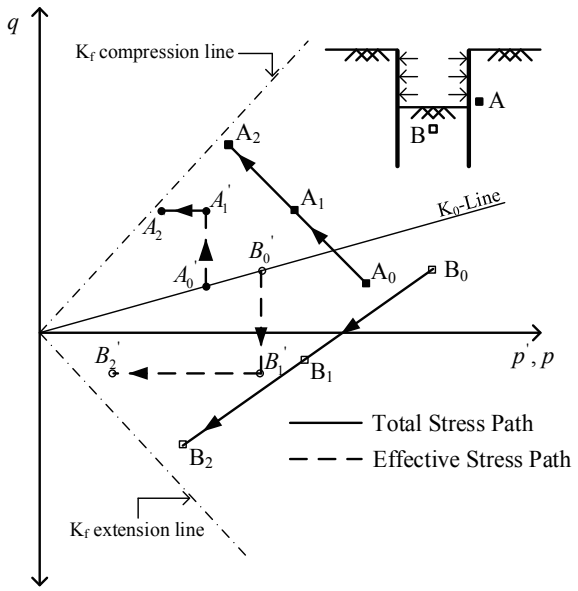

Fig. 1 Possible stress paths in excavations (Ng 1999)

undrained material can be conducted with effective stress undrained analysis or total stress undrained analysis. The commonly used effective stress model and total stress undrained model will be introduced in the following sections.

3.1 Effective Stress Model

Diaz-Rodriguez *et al*. (1992) studied the yield behavior of natural clays in different areas, in which the effective friction angle ranges from 17.5° to 43° (Fig. 2). The shape of the yield surface should be strongly influenced by the geological formation and constitutions of soil because it changes from areas to areas. As shown in Fig. 2, when values of the friction angle are low, the yield surfaces are in a flat shape. With the increase of the friction angle, the yield surfaces rotate upward and become thick and chunky. If $K_0 = 1 - \sin\phi'$ is assumed, the yield surface seems to be asymmetric with respect to the K_0 line because the upper part of the yield surfaces above the K_0 line appears to be fatter than the lower part. However, for simplification, the elliptical shape of the yield surface, symmetric with respect to the K_0 line, is often assumed for most of constitutive models of soil.

Figure 3 compares the yield surface of the typical Taipei silty clay, as established by Chin *et al*. (1994), with those predicted by the Modified Cam-clay (abbreviated as MCC, Roscoe and Burland 1968), MIT S1 (Pestana and Whittle 1999), RANI (Ou *et al*. 2011), and S-CLAY1 (Wheeler *et al*. 2003) models, in which the effective friction angles are assumed to be 30°. All of the yield surfaces are elliptical in shape. The MCC model obviously predicts the yield stress far from the test data. The yield stresses predicted by the MIT S1, RANI and S-CLAY1 models are generally in good agreement with the test data above the K_0 line and the S-CLAY1 model obtains the yield stress closer to the right part of the test data.

The MCC model is based on the critical state theory and originally means to simulate the behavior of normally and near-normally consolidated clays under triaxial compression test conditions. The yield surface of the MCC model in the p-q stress

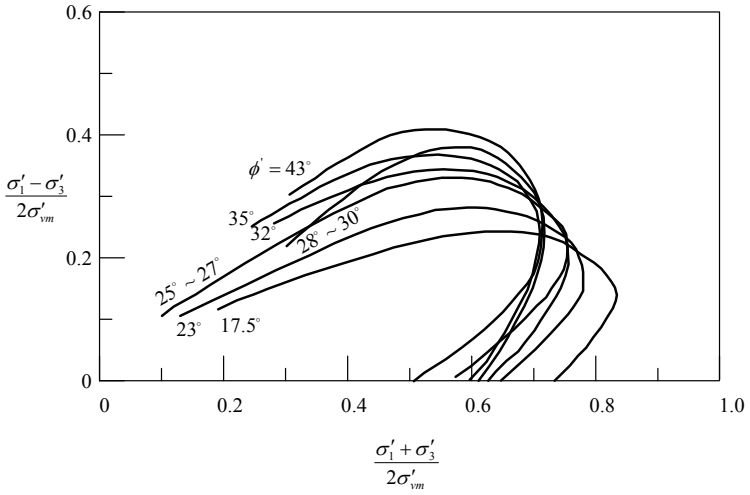

Fig. 2 Yielding surfaces of natural soils (Diaz-Rodriguez *et al.* 1992)

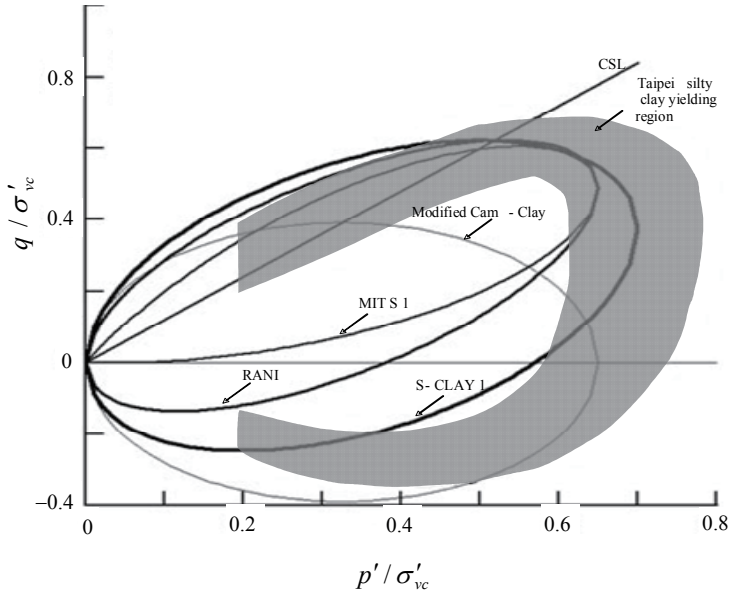

Fig. 3 The yield surface of the Taipei silty clay from tests and those predicted from various models

space is ellipse in shape and symmetric with respect to the hydrostatic line. The modified Cam-clay constitutive model involves five parameters, *i.e.*, the frictional constant, M, the isotropic logarithmic compression index, λ, the swelling index, κ, pure elastic or unloading-reloading Poisson's ratio, μ_{ur}, and pure elastic or unloading-reloading Young's modulus, E_{ur}. The yield surface is mainly determined by the parameter λ and M. The E_{ur}, a key parameter to control computed movements of excavations, can be derived from the swelling index κ (Lim *et al*. 2010).

Figure 4 shows the comparison of measured wall displacements of the TNEC case and those computed using the MCC model with the parameters directly from the laboratory tests, that is, real soil parameter (Lim *et al*. 2010). The wall displacements are close to field measurements at early stages (stages 1 and 2) while the computed wall deflections are smaller than the field measurements for intermediate to final stages. This can be explained by the fact that the MCC yield surface is symmetric to the hydrostatic line and the real soil yield surface is symmetric to the about K_0 line (Fig. 3). At the early stages, the soil is subjected to small unloading force, causing the stress state to be the inside of the MCC yield surface, and meanwhile also the inside of the real soil yield surface as predicted by S-CLAY1 model. The deformation behavior predicted by the MCC model thus matches the real behavior. This is why the wall displacement prediction curves are close to the field measurements at early stages. When excavation advances deeper, *i.e.*, intermediate to final stages, the unloading force was large enough to cause the stress state of the soil to be in the plastic state, *i.e.*, path A-B-C-E and relative large deformation occurs (Fig. 3). However, the stress state predicted from the model may be still inside the MCC yield surface. Hence, the computed wall displacements are smaller than the field measurements.

To obtain better analysis results, the parameter κ, directly related to movements induced by unloading force, should be adjusted. Considering that use of the MCC model may cause the normally consolidated soil in front the wall to be in the plastic state while the overconsolidated soil may be still in the elastic state, we therefore raise the κ-value from the original value (0.1 ~ 0.15)λ to 0.25λ for the soil at the depth of 12 ~ 37.5 m (normally consolidated clay) while the κ-value of the soil at the depth of 0 to 12 m (overconsolidated clay) remains unchanged. The rest of the input parameters remain to be unchanged. Figure 5 shows the comparison of measured wall displacements and those computed using the MCC model with the adjusted parameters. The computed wall displacements generally agreed with the field measurements.

Both Figs. 4 and 5 show that the computed surface settlements were much smaller than the field measurements for the soil near the wall but larger than the field measurements for the soil far away from the wall. This is attributed to the fact that the small strain characteristics are not considered in the MCC model.

The Hardening Soil model (abbreviated as the HS model, Schanz *et al*. 1999), is a true second order model for soils in general. The HS model requires 9 parameters, *i.e.*, three reference stiffness parameters (E_{50}^{ref} for triaxial compression, E_{ur}^{ref} for triaxial unloading/reloading or elastic Young's modulus, E_{oed}^{ref} for oedometer loading) at a reference stress level p^{ref}, a power, m, for the stress dependent stiffness formulation, the pure elastic Poisson's ratio or unloading/reloading Poisson's ratio, μ_{ur}, the Mohr-Coulomb strength parameters (ϕ, c), the K_0-value in primary one-dimensional compression (K_0^{nc}), and failure ratio, R_f. E_{ur}^{ref} is a key parameter to influence the movements of excavations. For undrained clay, the E_{ur}^{ref} can be determined from the swelling index κ, exactly the same as that in the MCC model (Lim *et al*. 2010). For sand, the E_{ur}^{ref} can be determined from the SPT (standard penetration test) correlation (Khoiri *et al*. 2014).

Figure 6 shows the comparison of the measured wall displacements and those computed by the HS model for the TNEC case. The computed wall displacements were generally close to the field measurement. Compared with the MCC model, the HS model gives better computed ground surface settlements. The HS model may be suitable for the analysis of deep excavation problems.

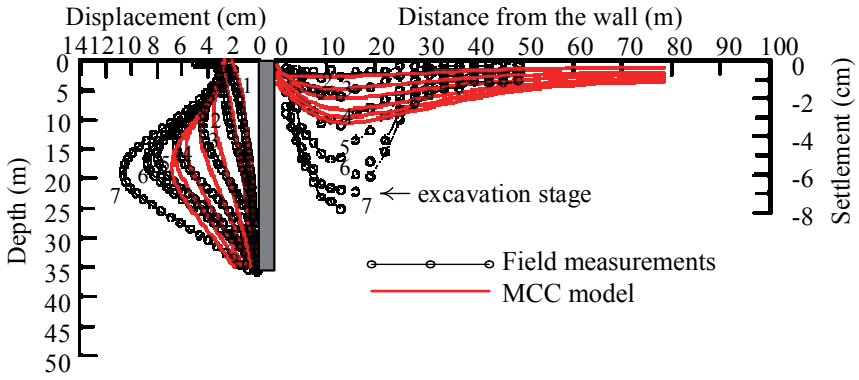

Fig. 4 The comparison of measured wall displacement and ground settlement profile with computed using the MCC model (real soil parameters)

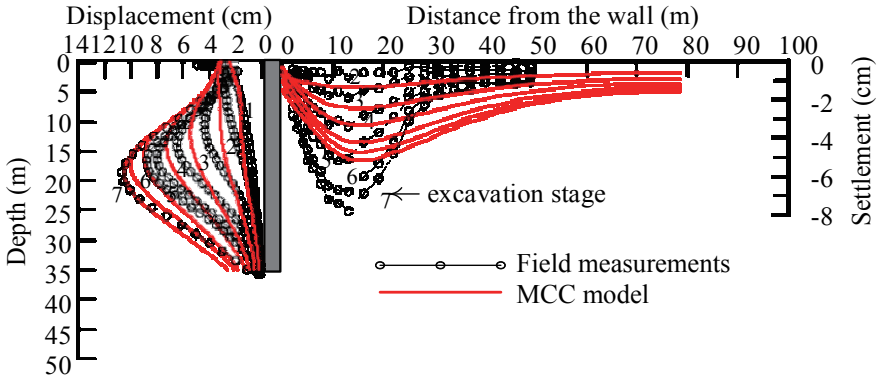

Fig. 5 The comparison of measured wall displacement and ground settlement profile with computed using the MCC model (adjusted parameter, $\kappa/\lambda = 0.25$)

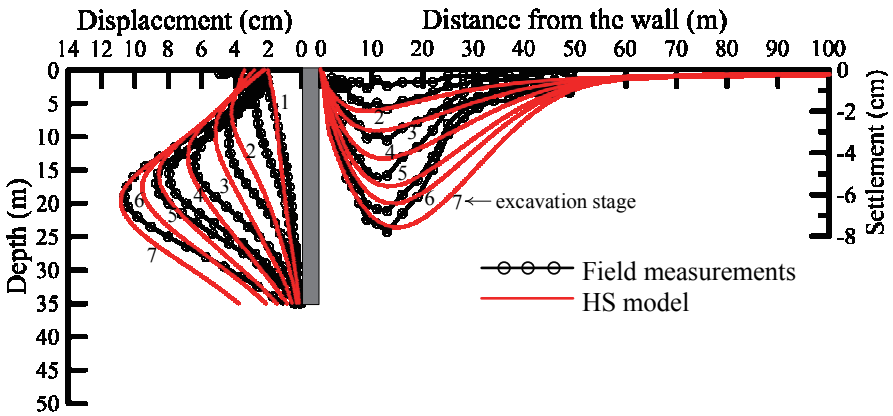

Fig. 6 The comparison of measured wall displacement and ground settlement profile with computed using the HS model

The hardening soil small strain model (abbreviated as HS small model, Benz *et al*. 2009) evolves from the hardening soil model with the consideration of small strain characteristics of soil. In the HS small model, two additional parameters are required: The reference shear modulus at small strain (G_0^{ref}) and shear strain ($\gamma_{0.7}$) at which the secant shear modulus equal to 0.7 G_0^{ref}. For analysis, the G_0^{ref} can be obtained from the bender element test and the $\gamma_{0.7}$ can be set equal to 10^{-5}. Figure 7 shows the analysis results using the model with $\gamma_{0.7} = 10^{-5}$. Compared with the results by the HS model (Fig. 6), the HS small model does not have a good effect in improving the analysis accuracy. The wall displacements computed from the HS small model for all stages were generally close to those from field measurements. The HS small model gives slightly better prediction in surface settlements though the prediction results are still far from the field measurements.

Lim and Ou (2016) has studied various stress paths of the soil in an excavation with the analysis of the TNEC case using the HS model. As shown in Fig. 8, the typical stress paths all moved vertically, either exceeding the initial shear yield surface

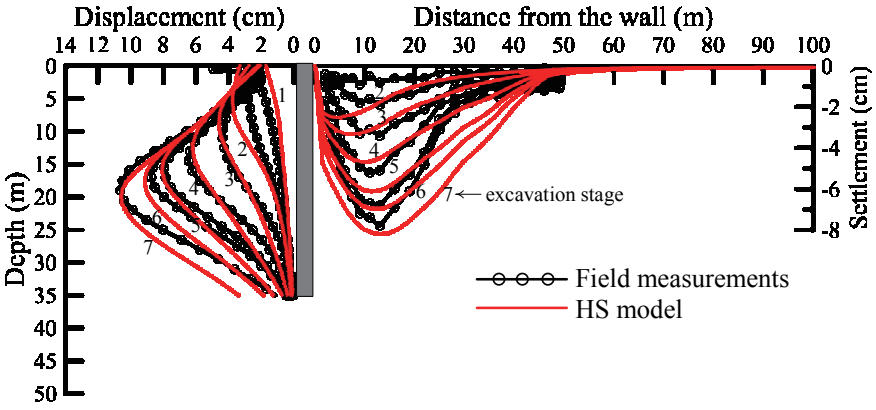

Fig. 7 The comparison of measured wall displacement and ground settlement profile with computed using the HS small model

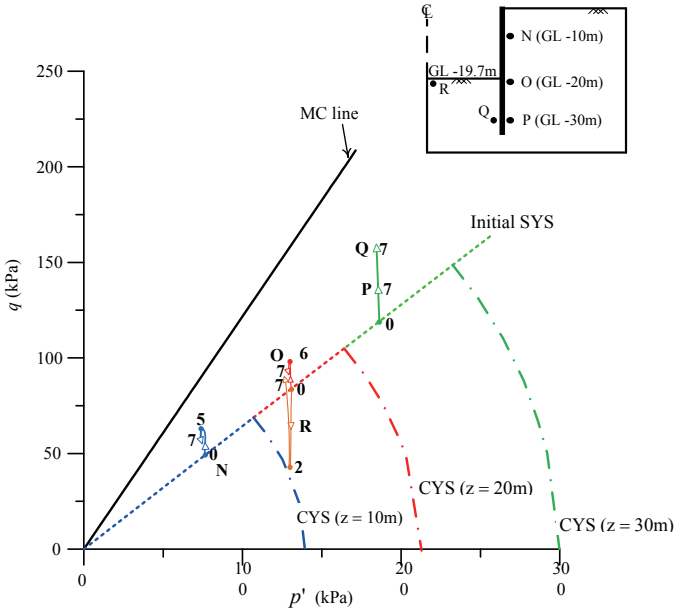

Fig. 8 Effective stress paths in the retained and excavated sides (note: CYS denotes cap yield surface; SYS denote shear yield surface)

(SYS) (points N, O, P and Q) but still inside the cap yield surface (CYS), or inside the initial shear yield surface and cap yield surface (point R). Results from finite element analysis also found that the change in the volumetric strain along those typical stress paths was almost equal to 0 and the generation of plastic volumetric strain (ε_v^p) was very small, around 10^{-5} when the soil yielded, *i.e.*, exceeding the initial shear yield surface. It was therefore proved that when the state of stress has not yet reached to the failure line, the soil was mainly dominated by elastic behavior. The unloading/reloading modulus should be recognized as a critical parameter in controlling deformation behavior of an excavation.

Therefore, the MC model were able to simulate the deformation behavior of the soil in excavations under the undrained condition. Since the MC model is unable to predict the nonlinear behavior of soil before failure, it would underestimate the generation of the excess porewater pressure under the undrained condition and thus overestimates the undrained shear strength (Fig. 9) if the effective strength parameters are applied (the MC undrained A approach). On the other hand, if the same effective unloading/reloading deformation parameters are used but the undrained shear strength was specified, *i.e.*, s_u and $\phi = 0$ as the strength parameters (Fig. 9(c)), the analysis is referred to as the MC undrained B approach. As featured in Fig. 10, the computed wall deflections obtained from the MC Undrained A and Undrained B diverse each other. At the final stage of excavation, the results from the MC Undrained B approach agree well with those from the HS model, even closer to the field measurements. The MC Undrained A resulted in smaller wall deflections as compared to those from the MC Undrained B because the MC Undrained A overestimates the undrained shear strength of clay.

The MC model is certainly applicable to the analysis of excavations in drained material like sand/gravel. Research has proved that Mohr-Coulomb model is applicable to sand sandy soil as long as appropriate selection of the stiffness parameters (Khoiri *et al*. 2014).

3.2 Total Stress Model

The $\phi = 0$ MC model is a total stress model, which involves four parameters, namely, the undrained strength parameters (c, ϕ) and the undrained deformation parameters (E_u, μ_u). With the total stress analysis, the undrained Poisson's ratio μ_u should be equal to 0.5 for the saturated clay under the undrained condition and the cohesion intercept should be equal to the undrained shear strength s_u and $\phi = 0$. The undrained elastic Young's modulus, E_u, should be determined based on empirical correlations or from back analysis of well-documented case histories. As long as an appropriate selection of Young's modulus, the wall deflection can be predicted with a good accuracy. Figure 11 shows the comparison of wall deflection from the field measurement with those from the MC model where the undrained Young's modulus was assumed to be equal to 500 s_u. Similar to the MCC model and HS model, the MC model is unable to predict the surface settlement well.

The undrained soft clay model, abbreviated as the USC model, is a stress path dependent total stress model, which considers the following characteristics of soil (Hsieh and Ou 2012):

1. Variation of undrained shear strength with principal stress rotation;
2. Variation of Young's modulus with the increase of stress level;

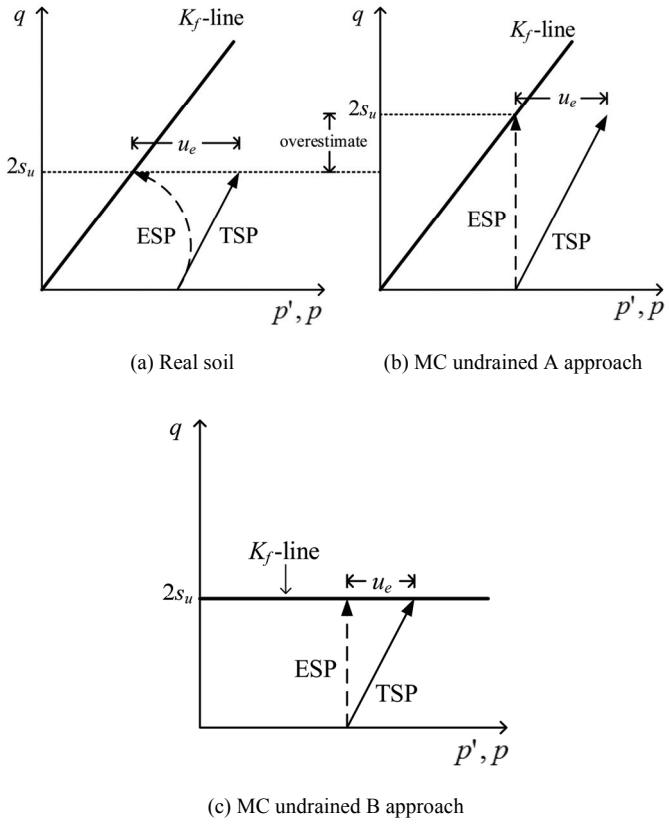

(a) Real soil (b) MC undrained A approach

(c) MC undrained B approach

Fig. 9 Effective and total stress paths of the soil subject to compression

3. High stiffness of soil at small strain;
4. Rational way to determine the undrained shear strength.

The USC model also employed the concept of the yield surface to differentiate the Young's modulus between the primary loading and unloading/reloading states. The unloading/reloading Young's modulus, E_{ur}, also degrade, from the range of small strain, with the increase of strain or stress level due to the development of pore water pressure.

Figure 12 compares the wall displacements from field measurement with those predicted from the USC model. The computed wall deflections for all stages agreed well with the field observations. The development of the wall deflection shape with the construction sequence and the location of the maximum wall deflection computed from the model were also very close to those observed in field observations. The computed surface settlements were also in good agreement with the observed settlements. The location of the maximum surface settlement computed from the model was almost the same as that from field observations. The USC model predicted both wall deflection and surface settlement well.

4. STABILITY ANALYSIS AND FAILURE MECHANISM OF EXCAVATIONS

The stability of deep excavations is a main concern for practical engineers. The failure of excavations is often characterized by the collapse of the support system and the large inward movement of the surrounding soil. Conventional methods, including Terzaghi's method, Bjerrum and Eide's method, and the slip circle method, are commonly used for the evaluation of basal heave stability of excavations in soft clay. In these methods, a failure surface of soil is first assumed, and the factor of safety (FS) against basal heave is then calculated as the ratio of the resistant force to the driving force. Although this calculation procedure is convenient for practical application, the actual failure surface may not be the same as that assumed in the conventional methods. Moreover, the methods are unable to identify if the failure is due to the soil or structures.

The stability of excavations has been studied by many researchers using the finite element method (FEM) with reduced shear strength (*e.g.*, Goh 1990; Faheem *et al.* 2003; Do *et al.* 2013). However, all of the previous studies used the elastic support system and did not model the existence of center posts in excavations that are used to support the horizontal struts, such that the FEM might not sufficiently simulate the behaviors of excavations. It is found that the factor of safety are overestimated.

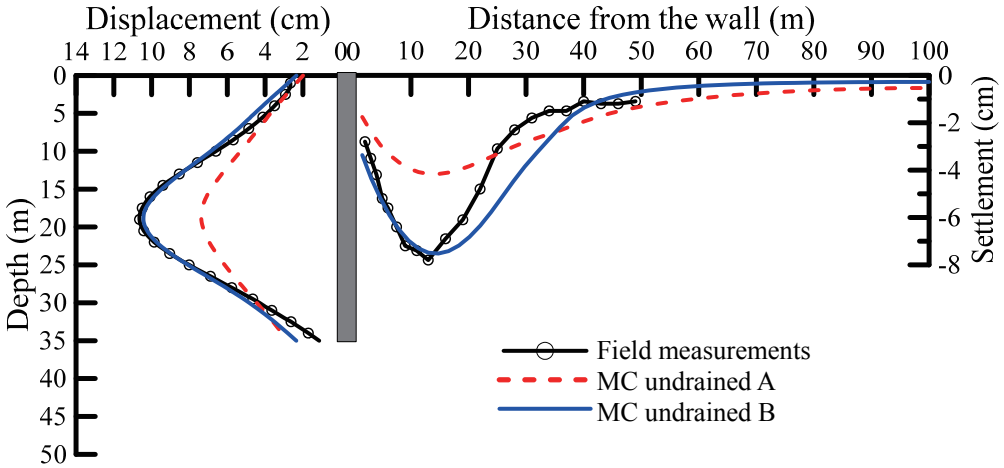

Fig. 10 The comparison of measured wall displacement and ground settlement profile with computed using the MC undrained A and B approached, respectively

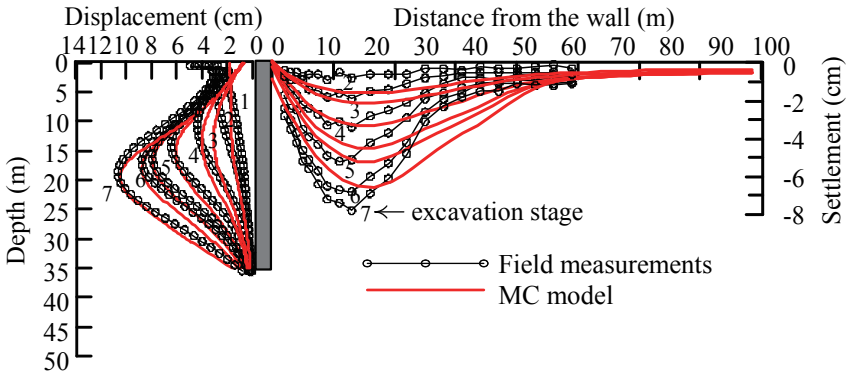

Fig. 11 The comparison of measured wall displacement and ground settlement profile with computed using the $\phi = 0$ MC model ($E/s_u = 500$)

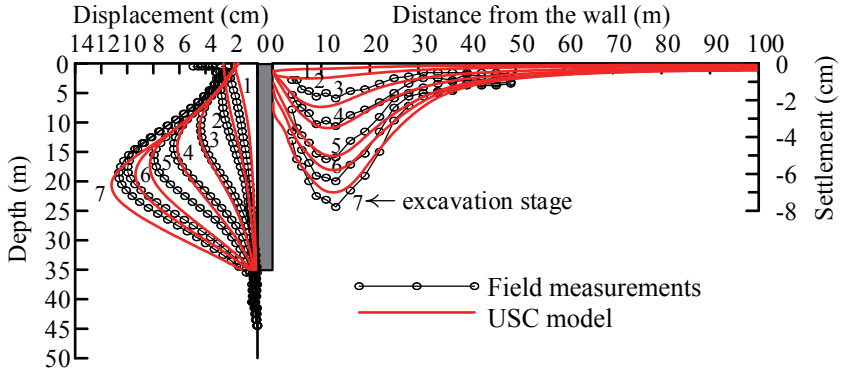

Fig. 12 The comparison of measured wall displacement and ground settlement profile with computed using the USC model

The author and his group furthermore performed the stability analysis of four failure cases in which the retaining wall and lateral supports were simulated with the elastic-plastic behavior and the center posts were considered in the finite element model (Do *et al*. 2016). The four cases are the Taipei Rebar Broadway excavation, the Taipei Shi-Pai case, the Hangzhou subway excavation and the Nicoll highway excavation. It is found that the factors of safety computed from the finite element was close to or smaller than 1.0 for all failure cases. The yielding of the struts or walls first caused a rapid increase in the wall deflection and soil heave and then the failure of the excavations. Figure 13 gives the wall deflection and soil heave at the excavation bottom at the final stage for different values of $\sum M_{stage}$ for the Taipei Rebar Broadway case where $\sum M_{stage}$ is the ratio of the unloading applied successfully in calculation to that caused by excavation at the final stage. The maximum strength reduction ratio was found incidentally to be 1.00 when excavation reached to the final stage, which also corresponds to the $\sum M_{stage\ max}$ value of 1.00. When excavation approached to the failure, the wall exhibited a kick-out deflection mode, and the maximum deflection (up to 400 mm) occurred at the wall toe. The soil heave also exhibited a consistent deformation mode, where the maximum heave (up to 500 mm) developed at the center of the excavation.

Figure 14 shows an interaction diagram of the internal forces (M, N) of the struts and walls in the finite element analysis where the support system was assumed to be elastic-plastic. The behaviors of the struts and walls are elastic when their internal force curves develop within the corresponding areas enveloped by the boundary lines that were constructed from the values of

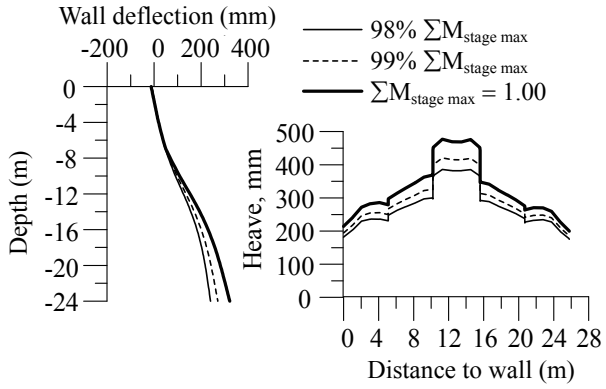

Fig. 13 Wall deflection and soil heave of Taipei Rebar Broadway case as using the elastoplastic support system

the plastic bending moment (M_p) and axial force (N_p). During excavation, the internal force curves of the struts at the first and second layers tended to develop toward the horizontal (M) axis. Their behaviors were significantly affected by the bending moment. On the other hand, the curves of the struts at the third layer grew toward the vertical (N) axis, indicating a higher impact of the axial force on this layer than the bending moment. The struts at the second and third layers started to yield at the fourth excavation stage. The struts at all the four layers yielded in the final excavation stage. In addition, the internal forces of the struts at the fourth (lowest) layer appeared at the topmost crest of the area enveloped by the boundary lines in this stage. This showed a predominant impact of the axial force on this layer, and therefore, the development of plastic hinges along the strut lengths could be inferred.

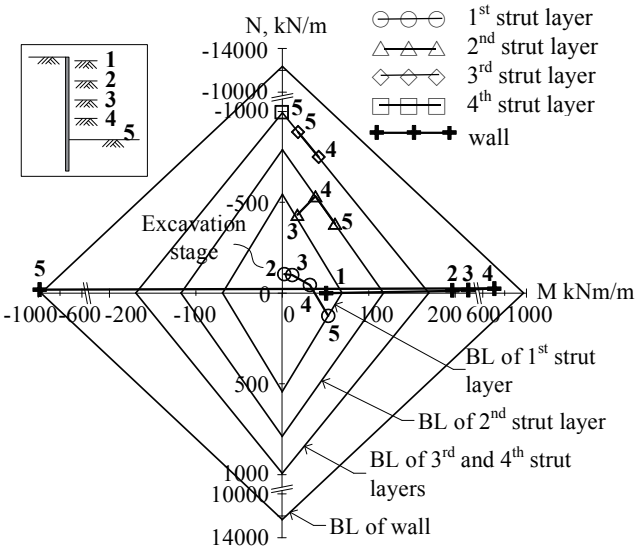

Note:
BL represents boundary lines.
At the 5th stage, internal forces corresponding to $\sum M_{stage\ max}$ are plotted.

Fig. 14 Interaction diagram of internal forces of elastic-plastic structural elements of Taipei Rebar Broadway case

In addition, the FEM analysis of other three cases were also performed and the factors of safety were also less than 1.0. It is also found that the yield or failure of the excavations was initiated from either the struts or walls rather from the soil. The results from the FE analysis were consistent with the field observation.

5. THREE DIMENSIONAL ANALYSIS

To avoid the damage of adjacent buildings during excavation, it is necessary to adopt effective measures to limit thewall deflection or ground settlement. Ground improvement is a common measure to reduce the excavation-induced ground movements (*e.g.*, Gaba 1990; Liu *et al*. 2005; Parashar *et al*. 2007). Recently, cross walls and buttress walls have been used as the alternative measures widely. The author and his group have shown that use of cross walls in deep excavations can reduce the wall deflection to a very small amount (*e.g.*, Ou *et al*. 2006; Ou *et al*. 2011). Since the mechanisum of cross walls in reducin the movements has been understood, a relevent simplified analysis was developed (Hsieh *et al*. 2012). However, use of cross walls in a very wide excavation would be costly. Therefore, buttress walls have been adopted recently as an alternative of cross walls for the protection of adjacent buildings during deep excavation.

However, the mechanism of buttress walls in limiting the wall defleciton is very complicated. Some engineers employed the concept of ground improvement to design buttress walls, that is, the average strength and stiffness of the soil in the passive zone increased due to the buttress walls. Some treat buttress walls to function as *T*-beams as those in reinforced concrete structures, enhancing the capability of moment-resistance of the diaphragm wall and some used frictional resistance between two sides of the buttress wall and adjacent soil to provide additional resistance to against the movement of the diaphragm wall. To have a good design of buttress walls, it is necessary to perform finite element analysis or to understand the mechanism of buttress walls in reducing the wall deflection.

Figure 15 shows the Park-2001 project in Taipei. The diaphragm wall was 21 m in depth and 0.6 m in thickness. Figure 15(b) and 15(c) show the dimension and depth of the buttress walls. Final excavation depth was 8.6 m. Figure 15(c) shows the construction sequence and subsoil profile and the basic soil properties.

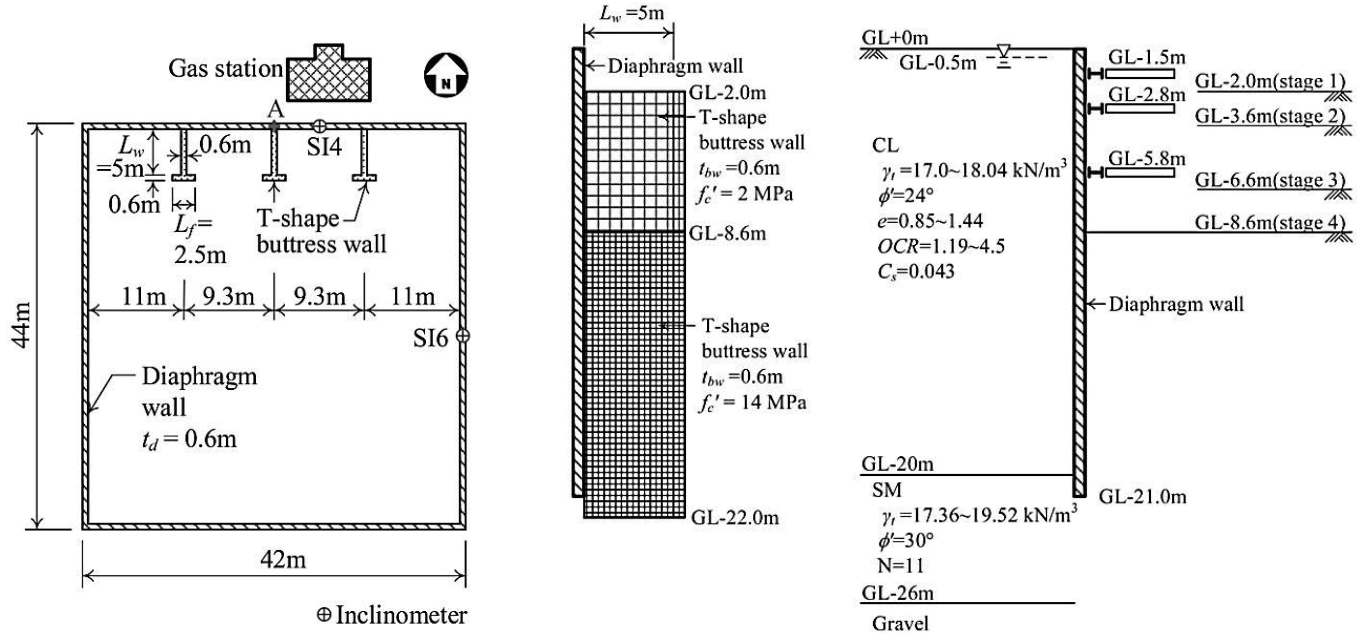

(a) Excavation plan (b) Types of buttress wall (c) Profile of the excavation

Fig. 15 The Park-2001 excavation project

Figure 16 plots a comparison of the computed and monitored wall deflections at SI4, near the location of a buttress wall using the HS model. The computed wall deflections were in general close to the monitored values but slightly overestimated at the last two stages. For the evaluation of effectiveness of buttress walls in reducing the wall deflection, analysis of the excavation with assumption of no buttress walls was performed and the results are also shown in Fig. 16. The computed maximum wall deflections with buttress wall and without buttress walls were 76.1 mm and 41.5 mm, respectively. Installation of buttress wall in this case certainly had good effects in reducing the wall deflection.

Figure 17 shows the computed wall deflections for the excavation where the retangular shape buttress walls, with the same area as the T-shape in the Park-2001 project, were employed. Results show that with consideration of frictional resistance between the buttress walls and the adjacent soil, the computed wall deflections were less than those for without buttress walls. The computed wall deflections for frictionless case were almost the same as those for without buttress walls. This implies that the main mechanism of the rectangular shape buttress walls in reducing the wall deflection was due to the frictional resistance between buttress walls and the adjacent soil. The combined bending stiffness of the diaphragm wall from the diaphragm wall and the rectangular shape buttress wall plays insignificant role in the reduction of the wall deflection. This is because when the buttress walls were demolished along with the removal of soil, the buttress walls below the excavation bottom were mainly "pushed" by the diaphragm wall rather than providing the bending resistance against the deformation of the diaphragm wall.

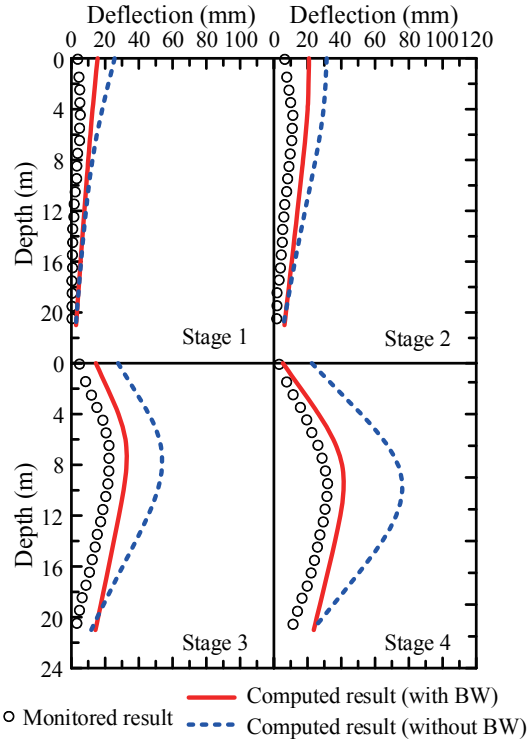

Fig. 16 Monitored and computed wall deflections at SI4 for the Park-2001 excavation project

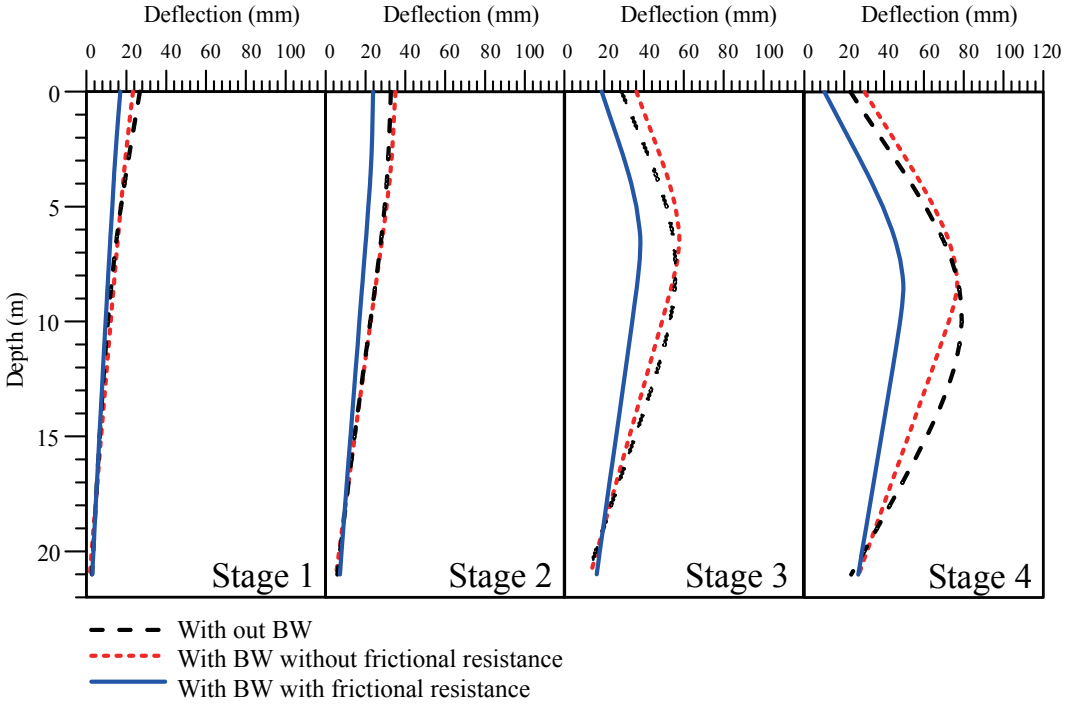

Fig. 17 Wall deflections for the assumed excavations without buttress walls and with buttress walls

To study the mechanism of buttress wall in reducing the wall deflection, the Park-2001 project was analyzed with the assumption of the retaingular shape of buttress walls with the lenght of 5 m, 10 m and 20 m, respectively. Figure 18 show the variation of the computed wall deflections for the scenarios with buttress walls and without buttress walls, respectively. The amount of wall deflection certainly decreased with the increasing length of buttress walls. To investigate the mobilization of shear strength, the relative shear stress ratio, τ_{rel}, is defined as the ratio of shear stress to the shear strength of a soil for a given effective normal stress. The $\tau_{rel} = 1.0$ implies that the soil adjacent to the buttress wall was at the failure state and its shear strength or frictional resistance was fully mobilized. Figure 19 illustrates the variation of the relative shear stress ratio on the surface of the buttress wall in the shallow excavation in clay and in sand, with the buttress wall length. The τ_{rel} was smallest near the diaphragm wall and generally increased with the increasing distance from the diaphragm wall, up to a value of 1.0. The τ_{rel} was mostly close to 1.0 for the short length of the buttress wall, *e.g.*, $L_r = 5$ m and majorly much less than 1.0 for the longer length of the buttress wall, *e.g.*, $L_r = 20$ m (Fig. 19).

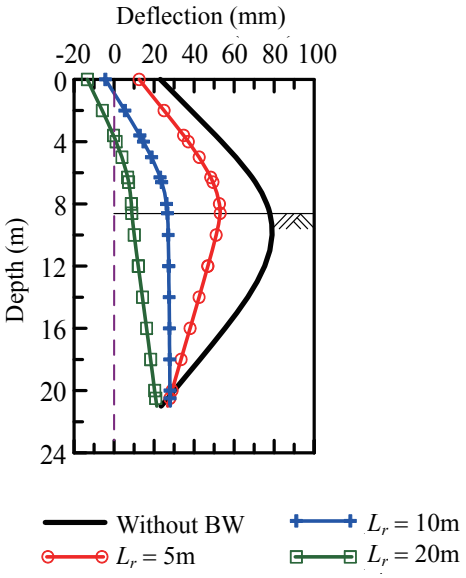

Fig. 18 Computed wall deflections for different lengths of the rectangular buttress wall in excavations

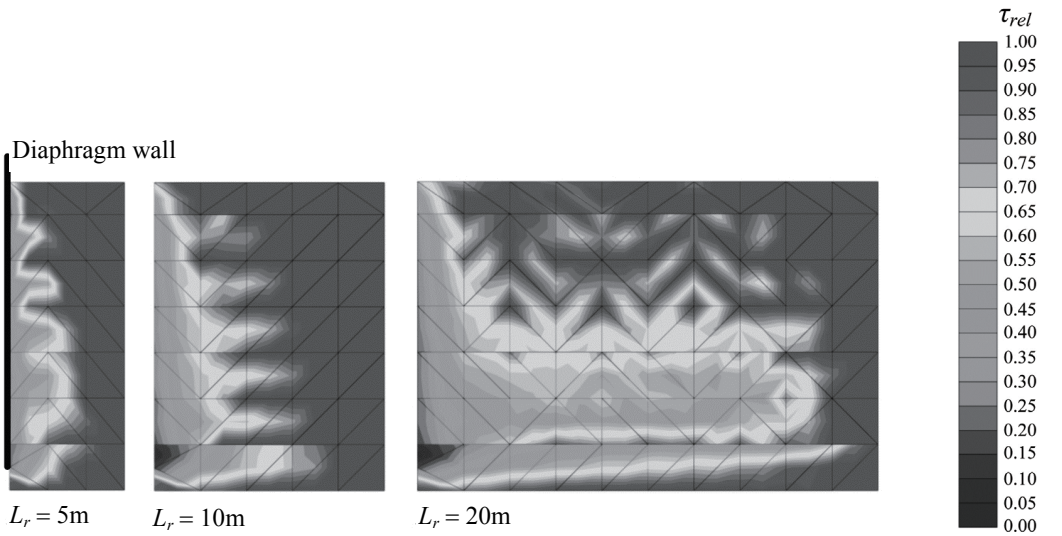

Fig. 19 Distribution of relative shear stress ratio for the cases with different lengths of the rectangular buttress wall

Figure 19 shows a relatively small shear stress ratio within the first 2.0 m from the diaphragm wall for all lengths of the buttress wall. This phenomenon can be explained by the fact that the movement at any location of the buttress wall was all the same, almost the same as the movement of the diaphragm wall. The soil in front of the diaphragm wall, say, 2.0 m from the diaphragm wall, directly pushed by the diaphragm wall, should have almost the same amount of movement as the diaphragm wall or buttress wall. Therefore, the relative displacement or relative shear stress ratio between the buttress wall and the adjacent soil within the first 2.0 m was very small but it increased gradually with the increasing distance from the diaphragm wall. It was clear that if the buttress wall length was less than 2.0 m, the buttress wall was unable to restrain the wall deflection although the combined bending stiffness from the contribution of the diaphragm wall and buttress wall seems increased.

6. CONCLUSIONS

The following conclusions can be drawn from the above studies:

1. The effective stress undrained analyses can generally result in good prediction of wall deflections for excavations in clay if the yield surface of the model and flow rule meet the deformation characteristics of soil. The input parameters can be derived from the basic properties of soil. However, the ground settlement cannot be predicted well unless the characteristics of high stiffness at small strain is incorporated in the constitutive model of soil. The total stress undrained model can also yield a good prediction of the movements in an excavation where the strength parameters of soil should be determined from laboratory or field tests but the Young's modulus can only be selected from empirical correlations.

2. For excavations under the undrained condition and normal construction, the soil in excavations is mostly dominated by elastic behavior. As long as the undrained shear strength can be specified, the effective stress MC model with $\phi = 0$ can result in good prediction of wall deflection.
3. Generally speaking, conventional formulae for stability analysis were derived from general bearing capability equations or simple force equilibrium. Though those have been used for decades, the mechanism of failure of excavations are unable to be found through those methods. Finite element method can be employed to estimate the factor of safety of excavations or investigate the mechanism of failure excavations when the wall and lateral supports can be simulated with the elastic-plastic behavior.
4. Ground improvement, cross walls and buttress walls are often designed to ensure the safety of adjacent buildings during deep excavation. Plane strain finite element analysis may be used to evaluate the performance of those measures but just to a certain extent. For some situations such as buttress walls where its interaction between structures and soil is complicated, three dimensional analysis is able to realistically evaluate the effectiveness of buttress walls in excavations. The mechanism of buttress walls in the reduction of wall deflection can also be investigated using the three dimensional finite element analysis.

ACKNOWLEDGEMENTS

The author acknowledges the research grants from the Ministry of Science and Technology in Taiwan (previously known as National Science Council) in the past. The results in this study mostly come from his supervised Master and PhD students. Their contributions in this paper are highly acknowledged.

REFERENCES

Benz, T., Vermeer, P. A., and Schwab, R. (2009). "A small-strain overlay model." *International Journal for Numerical and Analytical Methods in Geomechanics*, **33**, 25–44.

Bjerrum, L. and Eide, O. (1956). "Stability of strutted excavation in clay." *Geotechnique*, **6**(1), 32–47.

Bowles, J. E. (1986). *Foundation Analysis and Design*, McGraw-Hill, New York.

Chin, C. T., Crooks, J. H. A., and Moh, Z. C. (1994). "Geotechnical properties of the cohesive Sungshan Deposits, Taipei," *Geotechnical Engineering*, Southeast Asian Geotechnical Society, **25**(2), 77–103.

Clough, G. W. and O'Rourke, T. D. (1990). "Construction-induced movements of in situ walls." *Proceedings of the Design and Performance of Earth Retaining Structures*, ASCE Special Conference, Ithaca, New York, 439–470.

Diaz-Rodriguez, J. A., Leroueil, S., and Aleman, J. D. (1992). "Yielding of Mexico city clay and other natural clays." *Journal of Geotechnical Engineering*, **118**(7), 981–995.

Do, T. N., Ou, C. Y., and Chen, R. P. (2016). "A study of failure mechanisms of deep excavations in soft clay using the finite element method." *Computers and Geotechnics*, **73**, 153–163.

Do, T. N., Ou, C. Y., and Lim, A. (2013). "Evaluation of factors of safety against basal heave for deep excavations in soft clay using the finite element method." *Journal of Geotechnical and Geoenvironmental Engineering*, **139**, 2125–2135.

Faheem, H., Cai, F., Ugai, K., and Hagiwara, T. (2003). "Two-dimensional base stability of excavations in soft soils using FEM." *Computers and Geotechnics*, **30**(2), 141–163.

Gaba, A. R. (1990). "Jet grouting at Newton station." *Proceedings of the 10th Southeast Asia Geotechnical Conference*, Taipei, 77–79.

Goh, A. T. C. (1990). "Assessment of basal stability for braced excavation systems using the finite element method." *Computers and Geotechnics*, **10**(4), 325–338.

Hsieh, P. G., Ou, C. Y., and Liu, H. T. (2008). "Basal heave analysis of excavations with consideration of anisotropic undrained strength of clay." *Canadian Geotechnical Journal*, **45**, 788–799.

Hsieh, P. G. and Ou, C. Y. (1998). "Shape of ground surface settlement profiles caused by excavation." *Canadian Geotechnical Journal*, **35**, 1004–1017.

Hsieh, P. G. and Ou, C. Y. (2012). "Analysis of deep excavations in clay under the undrained and plane strain condition with small strain characteristics." *Journal of the Chinese Institute of Engineer*, **35**(5), 601–616.

Hsieh, P. G. and Ou, C. Y. (2016). "Simplified approach to estimate the maximum wall deflection for deep excavations with cross walls in clay under the undrained condition." *Acta Geotechnica*, **11**, 177–189.

Hsieh, P. G., Ou, C. Y., and Shih, C. (2012). "A simplified plane strain analysis of the lateral wall deflection for excavations with cross walls." *Canadian Geotechnical Journal*, **49**, 1134–1146.

JSA (1988). *Guidelines of Design and Construction of Deep Excavation*. Japanese Society of Architecture, Japan.

Khoiri, M., Ou, C. Y., and Teng, F. C. (2014). "A comprehensive evaluation of strength and modulus parameters of a gravelly cobble deposit for deep excavation analysis." *Engineering Geology*, **174**, 61–72.

Lim, A., Ou, C. Y., and Hsieh, P. G. (2010). "Evaluation of clay constitutive models for analysis of deep excavation under undrained conditions." *Journal of GeoEngineering*, **5**(1), 9–20.

Lim, A. and Ou, C. Y. (2016). *Stress Paths in Deep Excavations Under Undrained Conditions and Its Influence on Deformation Analysis*, Geotechnical Research Report GT1601, National Taiwan University of Science and Technology.

Liu, G. B., Ng, C. W. W., and Wang, Z. W. (2005). "Observed performance of a deep multistrutted excavation in Shanghai soft clays." *Journal of Geotechnical and Geoenvironmental Engineering*, **131**(8), 1004–1013.

Ng, C. W. W. (1999). "Stress paths in relation to deep excavations." *Journal of Geotechnical Engineering and Geoenvironmental Engineering*, **124**(5), 357–363.

Osman, A. S. and Bolton, M. D. (2006). "Ground movement predictions for braced excavations in undrained clay." *Journal of Geotechnical and Geoenvironmental Engineering*, **132**(4), 465–477.

Ou, C. Y. and Hsieh, P. G. (2011). "A simplified method for predicting ground settlement profiles induced by excavation in soft clay." *Computers and Geotechnics*, **38**, 987–997.

Ou, C. Y., Lin, Y. L., and Hsieh, P. G. (2006). "A case record of an excavation with cross walls and buttress walls." *Journal of GeoEngineering*, **1**(2), 579–86.

Ou, C. Y., Liu, C. C., and Chin, C. K. (2011). "Anisotropic visco-

plastic modeling of rate dependent behavior of clay." *International Journal for Numerical and Analytical Methods in Geomechanics*, **35**(11), 1189–1206.

Ou, C. Y., Hsieh, P. G., and Lin, Y. L. (2011). "Performance of excavations with cross walls." *Journal of Geotechnical and Geoenvironmental Engineering*, **137**(1), 94–104.

Parashar, S., Mitchell, R., Hee, M. W., Sanmugnathan, D., Sloan, E., and Nicholson, G. (2007). "Performance monitoring of deep excavation at Changi WRP project." *Proceedings of the 7th International Symposium on Field Measurements in Geomechanics*, Singapore, 1–12.

Peck, R. B. (1969). "Deep excavation and tunneling in soft ground." *Proceedings of the 7th International Conference on Soil Mechanics and Foundation Engineering*, State-of-the-Art Volume, Mexico City, 225–290.

Pestana, J. M. and Whittle, A. J. (1999). "Formulation of a unified constitutive model for clays and sands." *International Journal for Numerical and Analytical Methods in Geomechanics*, **23**, 1215–1243.

Roscoe, K. H. and Burland, J. B. (1968). "On the generalized stress-strain behavior of 'wet' clay." *Engineering Plasticity*, Heyman and Leckie, Eds., Cambridge University Press, Cambridge, 535–609.

Schanz, T., Vermeer, P. A., and Bonnier, P. G. (1999). "The hardening soil model: Formulation and verification." *Proceeding of Beyond 2000 in Computational Geotechnics—10 Years of PLAXIS*, Balkema, Rotterdam.

Terzaghi, K. (1943). *Theoretical Soil Mechanics*, John Wiley & Sons, Inc., New York.

Tschebotarioff, G. P. (1951). *Soil Mechanics, Foundations, and Earth Structures*, McGraw-Hill, New York.

Wheeler, S. J., Näätänen, A., Karstunen, M., and Lojander, M. (2003). "An anisotropic elasto-plastic model for natural clays." *Canadian Geotechnical Journal*, **40**(2), 403–418.